ResearchGate

See discussions, stats, and author profiles for this publication at: https://www.researchgate.net/publication/297678089

Multiobjective optimization using particle swarm optimization with non-Gaussian random generators

Article *in* Intelligent Decision Technologies · March 2016

DOI: 10.3233/IDT-150241

CITATIONS
0

READS
129

3 authors:

T. Ganesan
TNB Research Sdn. Bhd.
60 PUBLICATIONS **374** CITATIONS
SEE PROFILE

Pandian Vasant
Universiti Teknologi PETRONAS
219 PUBLICATIONS **1,492** CITATIONS
SEE PROFILE

Irraivan Elamvazuthi
Universiti Teknologi PETRONAS
186 PUBLICATIONS **1,039** CITATIONS
SEE PROFILE

Some of the authors of this publication are also working on these related projects:

converter View project

Ultrasound Imaging View project

All content following this page was uploaded by T. Ganesan on 10 March 2016.

The user has requested enhancement of the downloaded file.

Intelligent Decision Technologies 10 (2016) 93–103
DOI 10.3233/IDT-150241
IOS Press

Multiobjective optimization using particle swarm optimization with non-Gaussian random generators

T. Ganesan[a,*], P. Vasant[b] and I. Elamvazuthi[c]
[a]*School of Chemical Engineering, The University of Adelaide, Adelaide, SA, Australia*
[b]*Department of Fundamental and Applied Sciences, Universiti Teknologi Petronas, Tronoh, Perak, Malaysia*
[c]*Department of Electrical and Electronics Engineering, Universiti Teknologi Petronas, Tronoh, Perak, Malaysia*

AUTHOR COPY

Abstract. In engineering optimization, multi-objective (MO) problems are frequently encountered. In this work, a real-world MO problem (resin-bonded sand mould system) is tackled using Particle Swarm Optimization (PSO) in conjunction with the weighted-sum approach. Random generators (stochastic engines) provide sufficient randomness for the algorithm during the search process. The effects of non-Gaussian stochastic engines on the performance of the PSO technique in a MO setting is explored in this work. The stochastic engines operate using the Weibull distribution, Gamma distribution, Gaussian distribution and a chaotic mechanism. The two non-Gaussian distributions are the Weibull and Gamma distributions. The Pareto frontiers obtained were benchmarked using two metrics; the hypervolume indicator (HVI) and the proposed Average Explorative Rate (AER) metric. Detail comparative analysis on the effects of non-Gaussian random generators on the PSO technique is provided.

Keywords: Non-Gaussian random generators, multi-objective (MO) optimization, resin bonded sand mould system, particle swarm optimization (PSO), hypervolume indicator (HVI), average explorative rate (AER)

1. Introduction

Over the past years, MO optimization has been introduced and applied in many engineering problems. MO optimization problems are commonly tackled using the concept of Pareto-optimality to trace-out the non-dominated solution options on the Pareto curve (Zitzler and Thiele, 1998 [1]; Deb et al. 2002 [2]). Other methods include the weighted techniques which involve objective function aggregation resulting in a master weighted function (e.g. weighted sum approach [3] and the Normal Boundary Intersection technique [4]). In this work, the weighted-sum approach is employed to obtain the scalarized solutions. One of the most efficient approaches suitable for tackling complex optimization problems are swarm intelligence (SI) based techniques. This is mainly due to its effectiveness in the search process and its efficiency when it comes to computational time [5]. Some of the most common SI-based approaches are particle swarm optimization (PSO) [6], cuckoo search (CS) [7], ant colony optimization (ACO) [8] and bacterial foraging algorithm (PSO) [9,10].

In the past, one of the most popular technique employed for solving constrained nonlinear optimization problems is Particle Swarm Optimization (PSO) [6]. Particle Swarm Optimization (PSO) is an optimization method developed based on the movement and intelligence of swarms. PSO integrates the concept of social interaction to problem solving and decision-making. PSO was developed by James Kennedy and Russell Eberhart [6] in 1995. Particle swarm is the system model or social structure of a basic creature which makes a group to have some objectives such as food searching and predator-prey interactions. Hence, the

*Corresponding author: T. Ganesan, School of Chemical Engineering, The University of Adelaide, Adelaide 5005 SA, Australia. E-mail: tim.ganesan@gmail.com.

ISSN 1872-4981/16/$35.00 © 2016 – IOS Press and the authors. All rights reserved

governing principle is that it is an important to take part with the most of the population in a group that has the same activity. Recently, PSO has been applied to various fields of power system including economic dispatch problems as well as in optimization problems in electric power systems [11] and hybrid power plant design [12].

Over the past years, many research works have been directed towards resin bonded sand mould systems due to the following factors:

- Excellent adaptive capabilities in a dynamics environment.
- Good compliance to environmental factors.
- High casting quality [13].

This approach is power-saving and thus highly suitable for large-scale production [14]. In most cases, resin bonded sand mould systems show superb flow behaviour. Nevertheless some introduction of vibration and compaction during the moulding process is required. Casting properties are very much influenced by the mould properties (which are in effect dependent on the process parameters during mould development process) [15]. In this work, the multiobjective (MO) optimization model employed for the resin bonded sand system was developed in Surekha et al. [16]. This model was based on a resin bonded sand system where phenol formaldehyde was used as binder and tetrahydrophtalic anhydride was used as a hardener [16]. Since in this work, the problem formulation is MO in nature, PSO approach is utilized in tandem with the weighted-sum framework. Using this approach, multiple solutions are obtained for various weights which are then utilized to construct the Pareto frontier.

Most metaheuristic algorithms are endowed with a stochastic engine that generates random values which diversifies the algorithm's search space. These stochastic engines also provides the algorithm with a 'warm-start' priming it for the search operation. Therefore, the type of probability distribution function (PDF) that generates the random value in the stochastic engine heavily influences the algorithm's search capability. In most metaheuristic algorithms, the stochastic engine produces random numbers following a Gaussian PDF [17,18]. In other cases, researchers have employed other approaches to boost the stochastic engine by using chaos-based functions to couple with the Gaussian PDF [19]. These approaches avoid the algorithm from getting stuck in the local optima which causes premature convergence [20]. Thus, stochastic engines plays a crucial role in the implementation of metaheuristics. Besides Gaussian stochastic engines, another distribution that has rarely been investigated with respect to metaheuristics are the non-Gaussian distributions. These are usually heavy-tailed distributions, for instance; Gumbel [21], Weibull [22], Gamma [23] and Pareto [24] distributions. It has been known that many real-world systems (engineering, chemical or economic systems) do not behave in a stochastically Gaussian manner but are prone to contain non-Gaussian fluctuations.

The primary aim of this work is to analyse the effects of non-Gaussian stochastic engines on the performance of metaheuristics when implemented in a real-world engineering problem. In this work, the influence of the three types of stochastic engines (which are chaos-based, Gaussian-type PDF and Non-Gaussian-type PDF [25]) on the multiobjective optimization of the resin-bonded sand mould system. These approaches are compared and discussed in detail. The procedures are executed by the implementation of the PSO technique.

This paper is organized as follows: Section 2 introduces the Problem Description; Section 3 presents the four types of stochastic engines employed in this work while the PSO computational technique is included in Section 4. Section 5 provides detail discussions and analysis on the results obtained from the computational experiments. This paper ends with concluding remarks and recommendations for future research directions.

2. Problem description

The model describing the responses and the outputs of the optimization process was developed in Surekha et al. [16]. In that work, the mechanical properties of the quartz-based resin bonded sand core system was modelled using Mamdani-based fuzzy logic [26] and genetic algorithm [27] approaches. The multiobjective representation of the optimization model which consists of four objectives as developed in Surekha et al. [16] is as follows:

$$\begin{aligned} &\textit{Maximize} \rightarrow \textit{Permeability}, f_1 \\ &\textit{Maximize} \rightarrow \textit{Compression Strength}, f_2 \\ &\textit{Maximize} \rightarrow \textit{Tensile Strength}, f_3 \\ &\textit{Maximize} \rightarrow \textit{Shear Strength}, f_4 \\ &\text{subject to } \textit{process constraints.} \end{aligned} \tag{1}$$

The response parameters are; A, percentage of resin (%), B, percentage of hardener (%), C, number of

AUTHOR COPY

strokes and D, curing time (minutes). The final formulation of nonlinear regression model developed in Surekha et al. and the associated constraints are given as follows:

$$\begin{aligned} f_1 = {} & -333.77 + 614.73\mathrm{A} - 27.435\mathrm{B} \\ & +630.36\mathrm{C} - 18.97\mathrm{D} - 168.98\mathrm{A}^2 \\ & +0.239\mathrm{B}^2 - 76.08\mathrm{C}^2 + 0.111\mathrm{D}^2 \\ & +2.827\mathrm{AB} + 0.575\mathrm{AC} + 0.047\mathrm{AD} \\ & -0.7701\mathrm{BC}+0.1323\mathrm{BD}-0.1883\mathrm{CD} \end{aligned} \tag{2}$$

$$\begin{aligned} f_2 = {} & 2765.36 + 877.869\mathrm{A} - 112.778\mathrm{B} \\ & -731.934\mathrm{C} + 17.9222\mathrm{D} - 357.829\mathrm{A}^2 \\ & +0.983456\mathrm{B}^2+52.2310\mathrm{C}^2-0.0276946\mathrm{D}^2 \\ & +14.6571\mathrm{AB} + 96.8495\mathrm{AC}-3.74068\mathrm{AD} \\ & +7.62554\mathrm{BC}-0.096084\mathrm{BD}-1.27093\mathrm{CD} \end{aligned} \tag{3}$$

$$\begin{aligned} f_3 = {} & -354.406 + 211.418\,\mathrm{A} + 17.3611\mathrm{B} \\ & +96.7916\mathrm{C} + 2.78503\mathrm{D} - 44.7516\mathrm{A}^2 \\ & -0.173996\mathrm{B}^2-10.6696\mathrm{C}^2-0.026223\mathrm{D}^2 \\ & -2.08868\mathrm{AB}+6.05542\mathrm{AC}+0.197646\mathrm{AD} \\ & +2.07847\mathrm{BC}-0.078904\mathrm{BD}+1.18561\mathrm{CD} \end{aligned} \tag{4}$$

$$\begin{aligned} f_4 = {} & 318.163 + 726.696\mathrm{A} + 33.3432\mathrm{B} \\ & -721.381\mathrm{C} + 2.40622\mathrm{D} - 210.057\mathrm{A}^2 \\ & -0.189623\mathrm{B}^2+80.1788\mathrm{C}^2+0.000987\mathrm{D}^2 \\ & -1.89739\mathrm{AB}+49.8702\mathrm{AC}-0.32471\mathrm{AD} \\ & -1.70998\mathrm{BC}-0.07323\mathrm{BD}+0.306223\mathrm{CD} \end{aligned} \tag{5}$$

$$\begin{aligned} & A \in [1.5, 2.5], \quad B \in [30, 50], \\ & C \in [3, 5], \quad D \in [60, 100] \end{aligned} \tag{6}$$

3. Stochastic engines

3.1. Gaussian distribution

A random variable, $x \in X$ which is distributed with a mean, μ and variance, σ^2 is said to be a Gaussian or normally distributed when the PDF is as follows:

$$G_X(x) = \frac{1}{\sigma\sqrt{2\pi}} \exp\left[-\frac{1}{2}\left(\frac{x-\mu}{\sigma}\right)^2\right] \tag{7}$$

The Gaussian distribution is very general and widely applicable in various fields of studies for modelling real-valued random numbers (e.g. Brownian motion [28] and Monte Carlo simulations [29]). In this work, the standard normal distribution with $\mu = 0$ and $\sigma = 1$ is employed in the stochastic engine to generate random values in the metaheuristic.

3.2. Weibull distribution

The Weibull distribution is a type of non-Gaussian distribution which is widely implemented in extreme value statistics. A two-parameter Weibull distribution function for a random variable $x \in X$ is defined as follows:

$$W(x) = 1 - \exp\left[-\left(\frac{x}{\lambda}\right)^k\right] \text{ for } x \in R(0, +\infty) \tag{8}$$

where $W(x)$ is the Weibull distribution, k is the shape parameter and λ is the scale parameter. It is required that the scale and shape parameter are positive for the Weibull distribution ($k > 0$ and $\lambda > 0$). For $\lambda = 1$, the Weibull distribution takes the form of the exponential distribution. It should be noted that the Weibull distributions around λ gets smaller as the value of k increases. In this work, shape and scale parameters are set such that $\lambda = 1$ and $k = 5$. The Weibull distribution has been widely used in areas such as microbiology [30], information systems [31] and meteorology [32].

3.3. Gamma distribution

Similar to the Weibull distribution, the Gamma distribution is another type of non-Gaussian distribution. The Gamma distribution is influenced by its shape, α and rate, β parameters. The Gamma distribution, $\gamma(x)$ for a random variable $x \in X$ is given as follows:

$$\gamma(x) = 1 - \sum_{i=0}^{\alpha-1} \frac{(\beta x)^i}{i!} \exp(-\beta x) \text{ for } \forall i \in Z \text{ such that } \alpha > 0 \text{ and } \beta > 0 \tag{9}$$

The PDF of the Gamma distribution becomes near-symmetrical if there is an increment in the shape factor and the mean as the skewness decreases. As the standard deviation of the distribution increases, the PDF gradually skews to the left and becomes heavy-tailed. The Gamma distribution has been used successfully in climatology [33], insurance claim models [34] and risk analysis [35].

AUTHOR COPY

Table 1
PSO parameter settings

Parameters	Values
Initial parameter (c_1, c_2, r_1, r_2, w)	(1, 1.2, 0.5, 0.5, 0.8)
Number of particles	6
Initial social influence $(s_1, s_2, s_3, s_4, s_5, s_6)$	(1.1, 1.05, 1.033, 1.025, 1.02, 1.017)
Initial personal influence $(p_1, p_2, p_3, p_4, p_5, p_6)$	(3, 4, 5, 6, 7,8)

3.4. Chaotic generator

In this work, a one-dimensional chaotic map was used to initialize population of solutions by embedding the map into the random number generation component in the algorithm. The one-dimensional chaotic map, ψ_n is represented as the following:

$$\psi_{n+1} = f(\psi_n) \tag{10}$$

The most widely studied one-dimensional map is the logistic map [36] which is as the following:

$$f(\psi_n) = r_n \psi_n (1 - \psi_n) \tag{11}$$

$$r_{n+1} = r_n + 0.01 \tag{12}$$

where $\psi_n \in [0, 1]$ and $r_n \in [0, 5]$. In this mapping like all chaotic maps, the dynamics of the system varies for different sets of initial conditions (ψ_o and r_o).

4. Particle swarm optimization

In the study of agent-based algorithms, a swarm is a group of artificial organisms that behave interactively to achieve some pre-defined goal. This form of interaction gives the individuals in the swarm higher capabilities as well as better efficiency in achieving some arbitrary goal (as compared to a single individual). Many computational studies involving swarm intelligence have been conducted over the past years related to the flocking of birds, foraging of ants, motions of schools of fish, as well swarming of bees and wasps.

One such effective swarm intelligence approach is the PSO algorithm which was originally proposed by Kennedy and Eberhart [6]. This technique springs from two distinct frames of notions. The first notion was based on the investigation of swarming or flocking behaviours among some species of organisms (such as; birds, fishes, etc.). The second idea was inspired by the field of evolutionary computing. The PSO algorithm operates by exploring the search space for optimal candidate solutions and then evaluates these solutions with respect to some user defined fitness condition. The candidate optimal solutions obtained by this algorithm are achieved as a result of particles which are swarming through the fitness landscape. The velocity and position updating rule is critical to the optimization capabilities of this technique. The velocity and the position of each particle are updated using the following equations:

$$\begin{aligned} v_i(t+1) = w v_i(t) &+ c_1 r_1 [\hat{x}_i(t) - x_i(t)] \\ &+ c_2 r_2 [g(t) - x_i(t)] \end{aligned} \tag{13}$$

$$x_i(t+1) = x_i(t) + v_i(t+1) \tag{14}$$

where each particle is identified by the index i, $v_i(t)$ is the particle velocity and $x_i(t)$ is the particle position with respect to iteration (t). The terms, $c_1 r_1 [\hat{x}_i(t) - x_i(t)]$ and $c_2 r_2 [g(t) - x_i(t)]$ represent the personal and social influence respectively. These terms control the level of exploration and exploitation of the PSO algorithm during the search process in the objective space. The parameters w, c_1, c_2, r_1 and r_2 are usually defined by the user where these parameters are typically constrained with the following ranges:

$$\begin{aligned} &w \in [0, 1.2], \;\; c_1 \in [0, 2], \;\; c_2 \in [0, 2], \\ &r_1 \in [0, 1], \;\; r_2 \in [0, 1] \end{aligned} \tag{15}$$

The population size (maximum number of population), N_o and the maximum number of iteration, T is defined as well. The stopping criterion is satisfied when all particles/candidate solutions have reached their fittest positions during the iterations. The execution procedures of the PSO technique is given in the following pseudo code.

The parameter settings specified in the PSO variants employed in this work is shown in Table 1.

In the event the position of all the particles converges during the iterative process, the solutions are considered feasible. The solutions are considered feasible if the specified ranges are respected, no constraint violation exists, all the decision variables are non-negative and no further optimization of the objective function occurs. Therefore, based on these criteria it can be said that the fitness requirements have been met. The candidate solutions are hence at their fittest and in effect the program is stopped and the solutions are printed.

5. Measurement metrics

5.1. Hypervolume indicator

The Hypervolume Indicator (HVI) is a strictly Pareto-compliant indicator that is used to measure the qual-

AUTHOR COPY

START PROGRAM
Initialize no of particles, i and the algorithm parameters $w, c_1, c_2, r_1, r_2, N_o, T$
STOCHASTIC GENERATOR – Generate randomly located particles throughout the objective space
For $i = 1 \rightarrow N_o$ **do**
  Compute individual and social influence
  For $t = 1 \rightarrow T$ **do**
    Compute position $x_i(t+1)$ and velocity $v_i(t+1)$ at next iteration
    If swarm evolution time, $t > T$, **then** update position x_i and velocity v_i and update individual and social influence,
    Else proceed re-evaluate swarm fitness
    Evaluate fitness swarm
    If fitness criterion is satisfied, **then** halt program and print solutions,
    Else update individual and social influence,
  End For
End For
END PROGRAM

ity of solution sets in MO optimization problems [37, 38]. Strictly Pareto-compliant can be defined such that if there exists two solution sets to a particular MO problem, then the solution set that dominates the other would a higher indicator value. The HVI measures the volume of the dominated section of the objective space and can be applied for multi-dimensional scenarios. When using the HVI, a reference point needs to be defined. Relative to this point, the volume of the space of all dominated solutions can be measured. The HVI of a solution set $x_d \in X$ can be defined as follows:

$$HVI(X) = V\left(\bigcup_{(x_1,\ldots x_d)\in X} [r_1, x_1] \times \ldots \times [r_d, x_d]\right) \tag{16}$$

where $r_{1,\ldots,}r_d$ is the reference point and $V(\cdot)$ being the usual Lebesgue measure. In this work the HVI is used to measure the quality of the approximation of the Pareto front by the GSA and the DE algorithms when used in conjunction with the weighted sum approach.

5.2. Average explorative rate

The Average Explorative Rate (AER) is introduced in this work for the purpose of measuring the thoroughness of the search operation carried out by the computational technique in the regions of the objective space. The AER performs online measurements successively during the execution of the computational technique. This metric measures the amount of search region on average covered by the computational technique at each iteration. The proposed AER can be computed by first determining the deviation of the objective function values at each iteration:

$$\delta_n = \left[\frac{f^{n+1}(x_i) - f^n(x_i)}{f^n(x_i)}\right] \tag{17}$$

where $f^n(x_i)$ is the objective function value at the n^{th} iteration with x_i is the decision variables. Then the Heaviside Step Function is employed to return a value if the deviation, δ is more than some pre-defined value, L.

$$H(\delta_n) = \begin{cases} 0 \;\; if \;\; \delta_n < L \\ 1 \;\; if \;\; \delta_n \geqslant L \end{cases} \tag{18}$$

where $H(\delta_n)$ is the Heaviside Step Function. The AER (E_R) is then computed as follows:

$$E_R = \sum_{n=1}^{N} \left(\frac{H(\delta_n)}{N}\right) \tag{19}$$

where n is the iteration count and N is the maximum number of iteration. Therefore the larger the AER value, the more objective space is covered by the computational technique per iteration. This in effect results in a better search operation. It should be noted that when comparing computational techniques, the threshold value, L must be consistent throughout the computational experiments.

6. Computational results and analysis

Each of the four stochastic engines were imple-

AUTHOR COPY

Table 2
The individual solutions obtained using G-PSO

Description		Best	Median	Worst
Objective function	f_1	797.906	795.511	794.741
	f_2	804.544	792.045	788.719
	f_3	321.596	324.344	325.048
	f_4	425.084	417.108	414.799
Decision variable	A	1.83101	1.78298	1.77032
	B	30.5271	30.455	30.4361
	C	3.47888	3.41884	3.40301
	D	64.0494	63.5091	63.3667
Aggregated function	F	713.657	577.094	427.36

mented with the PSO technique. The PSO variants equipped with the Gaussian, Weibull and Gamma distributions are termed G-PSO, W-PSO and γ-PSO respectively. The PSO variant which is coupled to the random chaotic generator is called the Ch-PSO. The solutions obtained using the PSO variants are utilized to construct the approximate Pareto frontier. The algorithms employed in this work were programmed using the C++ programming language on a personal computer with an Intel® Core™ i5 processor running at 3.2 GHz. The entire Pareto frontier was constructed using 53 solutions at various weights attained for each of the PSO variants. The degree of dominance these solutions is measured using the HVI. The nadir point or the measurement reference in the HVI is $(q_1, q_2, q_3, q_4) = (0, 0, 0, 0)$. Each solution point obtained is selected by taking the best solution obtained from 10 independent runs of the algorithms (for each of the individual weights). The individual solutions for specific weights of the PSO variants were assessed based on the value of the aggregate objective function (weighted-sum approach):

$$F = \sum_{\forall i \in [1,4]} \beta_i f_i \tag{20}$$

where F is the aggregate objective function, f_i are the individual objective functions and β_j are the respective weights. Therefore the solutions may be ranked into four classifications (best, median and worst). The individual solutions for the G-PSO technique along with their aggregate respective values of the objective functions are given in Table 2.

For the best, median and worst solution are weights (w_1, w_2, w_3, w_4) are (0.7, 0.1, 0.1, 0.1), (0.1, 0.4, 0.3, 0.2) and (0.1, 0.1, 0.7, 0.1). The entire Pareto frontier constructed using the G-PSO approach is shown in Fig. 1.

The individual solution and the approximate Pareto frontier for the W-PSO technique is as shown in Table 3 and Fig. 2.

Table 3
The individual solutions obtained using W-PSO

Description		Best	Median	Worst
Objective function	f_1	977.129	976.923	977.168
	f_2	1000.93	1000.86	1000.94
	f_3	290.912	290.976	290.906
	f_4	461.961	461.982	461.96
Decision variable	A	2.49985	2.49949	2.49989
	B	45.5894	45.584	45.5903
	C	4.3758	4.37536	4.37588
	D	71.8783	71.8743	71.8788
Aggregated function	F	873.652	677.727	447.641

Table 4
The individual solutions obtained using γ-PSO

Description		Best	Median	Worst
Objective function	f_1	791.886	791.885	791.886
	f_2	778.003	778.002	778.004
	f_3	327.231	327.23	327.23
	f_4	406.835	406.833	406.835
Decision variable	A	1.72985	1.72984	1.72985
	B	30.3753	30.3753	30.3753
	C	3.3524	3.35239	3.3524
	D	62.9112	62.9111	62.9113
Aggregated function	F	705.527	572.701	426.734

Table 5
The individual solutions for the Ch-PSO approach

Description		Best	Median	Worst
Objective function	f_1	796.525	797.531	795.411
	f_2	796.911	802.349	791.663
	f_3	323.284	322.082	324.417
	f_4	420.339	423.757	416.839
Decision variable	A	1.80148	1.82241	1.78143
	B	30.4828	30.5143	30.4528
	C	3.44213	3.46829	3.41703
	D	63.7181	63.9535	63.4923
Aggregated function	F	711.698	581.105	427.483

The associated weights (w_1, w_2, w_3, w_4) for the best, median and worst solution provided by the W-PSO approach (refer to Table 2) are (0.1, 0.7, 0.1, 0.1), (0.1, 0.4, 0.3, 0.2) and (0.1, 0.1, 0.7, 0.1). The individual solutions for the γ-PSO approach are given in Table 4.

For the best, median and worst solution are weights (w_1, w_2, w_3, w_4) are (0.7, 0.1, 0.1, 0.1), (0.3, 0.2, 0.3, 0.2) and (0.1, 0.1, 0.7, 0.1). The entire Pareto frontier constructed using the γ-PSO approach is shown in Fig. 3.

The individual solutions for the Ch-PSO technique and the aggregate objective function values are given in Table 5. Figure 4 shows the entire Pareto frontier obtained using the Ch-PSO approach.

AUTHOR COPY

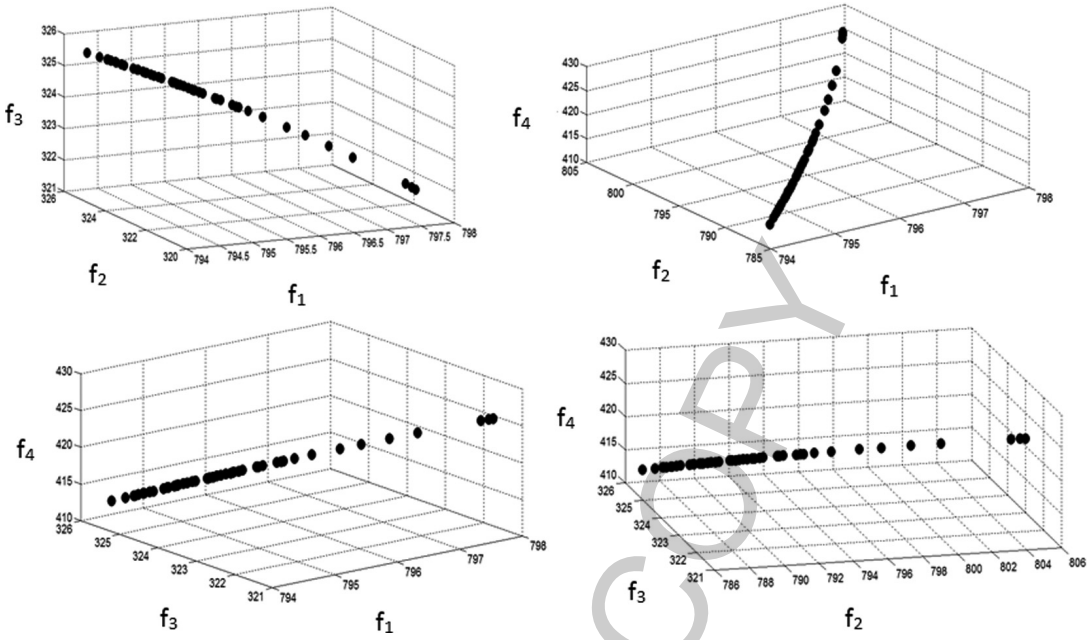

Fig. 1. Pareto frontier obtained using G-PSO.

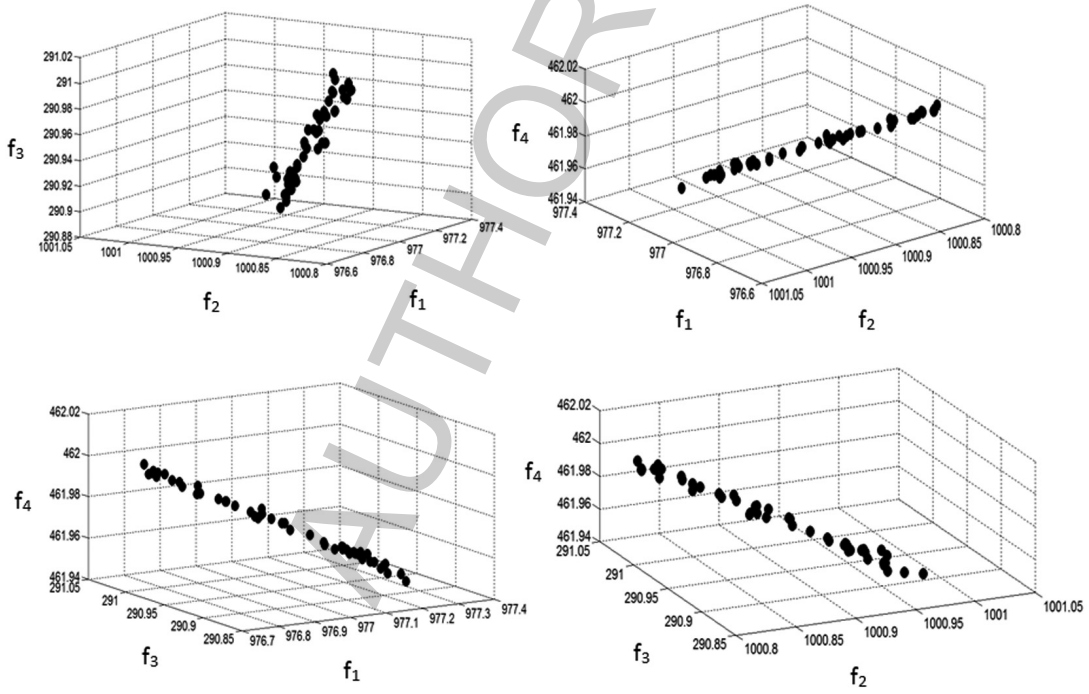

Fig. 2. Pareto frontier obtained using W-PSO.

The associated weights (w_1, w_2, w_3, w_4) for the best, median and worst solutions produced by Ch-PSO approach are (0.5, 0.3, 0.1, 0.1), (0.3, 0.2, 0.3, 0.2) and (0.1, 0.1, 0.7, 0.1). The overall dominance levels produced by HVI for each of the Pareto frontiers obtained using the PSO variants is shown in Fig. 5.

Figure 5 shows that the W-PSO generates the most dominant Pareto frontier. The second most dominant

AUTHOR COPY

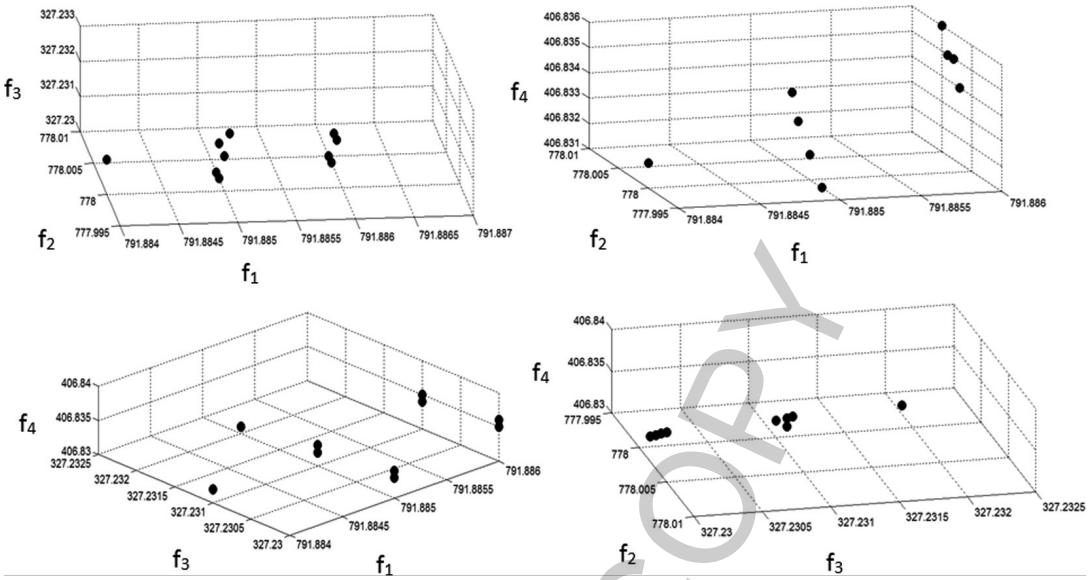

Fig. 3. Pareto frontier obtained using γ-PSO.

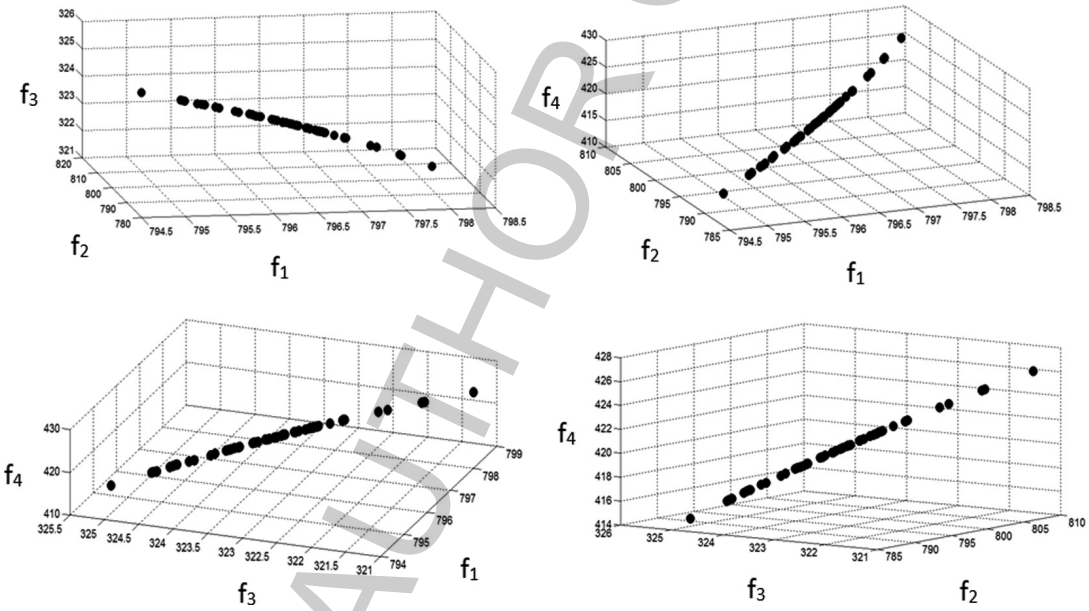

Fig. 4. Pareto frontier obtained using Ch-PSO.

AUTHOR COPY

frontier is obtained using the Ch-PSO followed by the G-PSO while the least dominant frontier was produced the γ-PSO. The frontier obtained using the W-PSO approach is more dominant than γ-PSO, G-PSO and Ch-PSO by 60.253%, 54.321% and 52.593% respectively.

In Fig. 2, the frontier produced by the W-PSO can be seen to have a good solution spread. The solutions in Fig. 2 are well-concentrated in highly optimal regions in the objective space. This critical feature makes the frontier obtained using the W-PSO more dominant as compared to all the other approaches employed in this work. The solutions in the frontiers produced by the G-PSO and the Ch-PSO (Figs 1 and 4) are seen to be very intense in some regions and rather sparse in other areas of the objective space. For instance, Fig. 1 shows that the solutions produced by the G-PSO are very sparsely spread at regions with high values of f_1, f_2, f_4 and low values of f_3. Regions with low values of f_1, f_2, f_4

Table 6
Comparison of the best individual solutions generated by the PSO variants

Description		W-PSO	ϒ-PSO	G-PSO	Ch-PSO
Objective function	f_1	749.885	791.886	797.906	796.525
	f_2	970.923	778.003	804.544	796.911
	f_3	273.725	327.231	321.596	323.284
	f_4	402.915	406.835	425.084	420.339
Decision variable	A	2.4999	1.72985	1.83101	1.80148
	B	31.559	30.3753	30.5271	30.4828
	C	4.37588	3.3524	3.47888	3.44213
	D	71.8789	62.9112	64.0494	63.7181
Aggregated function	F	822.299	705.527	713.657	711.698

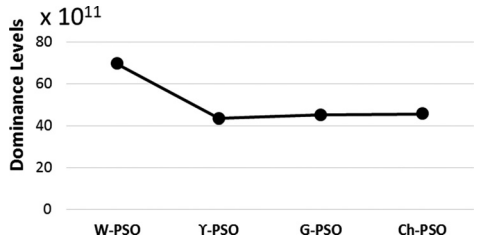

Fig. 5. Dominance levels for the Pareto frontiers.

and high values of f_3, have high concentrations of solutions produced by the G-PSO technique (Fig. 1). On the other hand, Fig. 4 shows that the Ch-PSO technique produces highly sparse solution spreads at the extreme ends of the values of all the objective functions. The solutions on the frontier are mostly concentrated on the midrange of the objective functions (Fig. 4). Due to this localized nature of the solutions produced by the G-PSO and the Ch-PSO (Figs 1 and 4), it is more likely that the solution points miss the optimal regions in the objective space. Thus, as compared to the W-PSO, the Pareto frontier produced by both the G-PSO and the Ch-PSO have inferior dominance levels. The frontier constructed using the γ-PSO is extremely conglomerated (although having excellent coverage) to very narrow regions of the objective space (Fig. 3). Thus, more of the optimal regions in the objective space are missed making the frontier by the γ-PSO the least dominant as compared to all the other techniques employed in this work. The individual solutions generated by the PSO variants are assessed using the value of the aggregate objective function similar to Tables 2–5. Table 6 shows the best individual solution produced by each of the PSO variants.

In Table 6, it can be observed that the individual solutions produced by the W-PSO are more optimal than the solutions produced by all other techniques employed in this work. The W-PSO outweighs the γ-PSO, G-PSO and Ch-PSO by 16.551%, 15.223% and

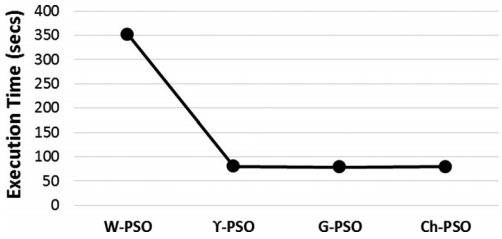

Fig. 6. Execution time for the PSO variants.

15.53% respectively. Figure 6 presents the execution time (in seconds) for each of the PSO variants. The execution time considered is the time taken for the technique to generate the entire Pareto frontier by taking using the individual solutions according to their respective weights.

In Fig. 6, the execution time for the W-PSO is the highest (325.156 secs) followed by γ-PSO (80.188 secs). The least search time was taken by the G-PSO (78.56 secs) and Ch-PSO (79.354 secs). It can be observed that in Fig. 6, the execution time taken by W-PSO far exceeds the other techniques employed in this work. The W-PSO takes a longer time since it engages in a very rigorous and thorough search operation as compared to the other PSO variants. This clearly reflects in the degree of frontier dominance achieved by the W-PSO as compared to the other variants (Fig. 5). Although the other techniques (γ-PSO, G-PSO and Ch-PSO) complete the computations fast, it is likely that they converge prematurely. Thus, their search efforts lack rigor such that they often miss the optimal/dominant regions in the objective space. It is important to note that the execution time in this case is directly influenced by the mechanisms of the search operation carried out by the technique and not related to the algorithmic complexity. In this work, the only difference between the PSO variants are the stochastic engines (PDF) utilized. Since the algorithmic complexity is not significantly affected by the difference in the stochastic engine, the execution time is related only to the efficiency of the search operation. The proposed AER metric was utilized to measure the rate of exploration carried out by each of the approaches. The values of the obtained AER are shown in Fig. 7.

Figure 7 shows the AER values for the PSO variants to produce the entire Pareto frontier. It can be observed that the highest AER value was attained by the W-PSO approach followed by the Ch-PSO, G-PSO and the γ-PSO respectively. The AER value is seen to be related to the dominance levels identified by the HVI for all the techniques (Fig. 5). Similarly the Pareto frontier

AUTHOR COPY

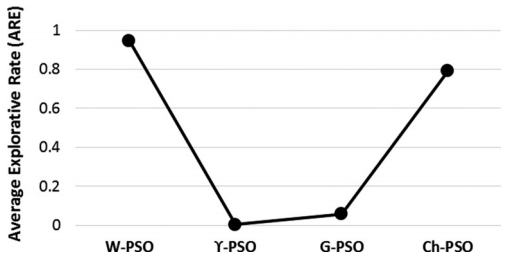

Fig. 7. AER value for the PSO variants.

generated by the γ-PSO has the lowest dominance and the lowest AER value. The explorative rate is an indicator of how well the technique explores the objective space during the search operation. This is effect influences the effectiveness of the approach in constructing a dominant Pareto frontier. The AER is very suitable to be utilized as an online metric since it does not require information from a completed search operation to be assessed. Therefore the AER may improve the adaptability of the algorithm by iterative evaluation/ correction procedures during execution. In this problem, the nadir point was chosen such that all the solution points produced by the PSO variants dominates this point. Thus, computational results evaluated using the HVI are independent of the nadir point selection. To handle the MO feature of this problem, the weighted-sum scalarization framework was employed. This framework was used to construct the Pareto frontier from the individual solutions along with their respective weightages. Although the weighted sum approach is very apt for Pareto frontier construction in multiobjective scenarios, this approach fails to guarantee Pareto optimality [39]. The only setback with scalarization techniques such as the weighted-sum approach is that they may fail to completely describe the Pareto frontier if they are concavely structured. In this work, the solution points obtained using the PSO variants were feasible and none of the constraints were violated. All computational approaches performed stable computations during program executions with no convergence issues.

7. Conclusions and recommendations

The concept of using non-Gaussian PDFs in place of the conventional Gaussian stochastic engine has yielded interesting results. Table 3 and Fig. 5 show that the W-PSO outranks all the other approaches employed in this work in terms of individual solution quality as well as in terms of Pareto frontier dominance. However, the γ-PSO which has a non-Gaussian stochastic engine performs poorly as compared to the W-PSO and the conventional G-PSO. These results show that having a non-Gaussian stochastic engine in a computational approach may be advantageous. Nevertheless, it is the choice of the distribution-type in the solution method may very well influence the algorithm's performance. In addition, the Non-Gaussian distribution type may also be correlated with the solution landscape. Due to this dependence, the effectiveness of the computational approach with a particular type of non-Gaussian stochastic engine would vary based on the problem characteristics and type. In these numerical experiments, the proposed AER metric was seen to correlate with other measurements carried out in this work. The AER metric could be employed in more computational approaches in future research works as an effective tool to direct the search effectively towards optimal regions in the objective space. In addition, other types of non-Gaussian distributions such the Gumbel distribution [21] could be tested as a stochastic engine in other types of optimization techniques. Besides, more real-world multiobjective problems [40,41] could be explored using computational techniques with non-Gaussian stochastic engines to investigate and validate the effectiveness of this framework in solving optimization problems.

AUTHOR COPY

References

[1] E. Zitzler, J. Knowles and L. Thiele, Quality assessment of pareto set approximations, Chapter 15, *Multiobjective Optimization*, J. Branke et al., eds, Springer-Verlag Berlin Heidelberg, (LNCS 5252), 2008, pp. 373–404.

[2] K. Deb, A. Pratap, S. Agarwal and T. Meyarivan, A fast and elitist multi-objective genetic algorithm: NSGA-II, *IEEE Transactions on Evolutionary Computation* **6**(2) (2002), 182–197.

[3] R.T. Marler and J.S. Arora, The weighted sum method for multi-objective optimization: New insights, *Structural and Multidisciplinary Optimization* **41**(6) (Jun 2010), 853–862.

[4] A. Zangeneh, S. Jadid and A. Rahimi-Kian, Normal boundary intersection and benefit – cost ratio for distributed generation planning, *European Transactions on Electrical Power* **20**(2) (2010), 97–113.

[5] Y. Liu, K.M. Passino and M.A. Simaan, Biomimicry of social foraging bacteria for distributed optimization: Models, principles, and emergent behaviors, *Journal of Optimization Theory and Applications* **115**(3) (2002), 603–628.

[6] J. Kennedy and R. Eberhart, Particle swarm optimization, *IEEE Proceedings of the International Conference on Neural Networks*, Perth, Australia (1995), 1942–1948.

[7] A.R. Yildiz, Cuckoo search algorithm for the selection of optimal machining parameters in milling operations, *International Journal of Advanced Manufacturing Technology* **64**(1–4) (2013), 55–61.

[8] W.F.A. El-Wahed, A.A. Mousa and M.A. Elsisy, Solving economic emissions load dispatch problem by using hybrid ACO-MSM approach, *The Online Journal on Power and Energy Engineering (OJPEE)* **1** (2008), 31–35.
[9] K. Passino, Biomimicry of bacterial foraging for distributed optimization and control, *IEEE Control Systems Magazine* **22**(3) (2002), 52–67.
[10] I.A.A. Al-Hadi and S.I. M Hashim, Bacterial foraging optimization algorithm for neural network lea rning enhancement, *International Journal of Innovative Computing* **1**(1) (2002), 8–14.
[11] N. Phuangpornpitak, W. Prommee, S. Tia and W. Phuangpornpitak, A study of particle swarm technique for renewable energy power systems, *PEA-AIT International Conference on Energy and Sustainable Development: Issues and Strategies* (2010), Thailand, 1–7.
[12] L. Wang and C. Singh, PSO-based multi-criteria optimum design of a grid-connected hybrid power system with multiple renewable sources of energy, *Proceedings of the IEEE Swarm Intelligence Symposium*, (2007).
[13] E. Ireland, K. Chang and J. Kroker, New horizon in no-bake binder technology, *AFS Transactions* **110** (2002), 1–7.
[14] W. Liu, Y. Li, X. Qu and X. Liu, Study on binder system of CO2-cured phenol-formaldehyde resin used in foundry, *China Foundry* **5**(2) (2008), 110–113.
[15] M.B. Parappagoudar, D.K. Pratihar and G.L. Datta, Non-linear modeling using central composite design to predict green sand mould properties, *Proceedings IMechE B Journal of Engineering Manufacture* **221** (2007), 881–894.
[16] B. Surekha, D. Hanumantha Rao, G. Krishna, M. Rao, P.R. Vundavilli and M.B. Parappagoudar, Modeling and analysis of resin bonded sand mould system using design of experiments and central composite design, *Journal of Manufacturing Science and Production* **12** (2012), 31–50.
[17] I. Elamvazuthi, T. Ganesan and P. Vasant, A comparative study of HNN and Hybrid HNN-PSO techniques in the optimization of distributed generation (DG) power systems, International Conference on Advanced Computer Science and Information System (2011), 195–200.
[18] T. Ganesan, I. Elamvazuthi, K.Z.K. Shaari and P. Vasant, Multiobjective optimization of green sand mould system using chaotic differential evolution, *Transactions on Computational Science XXI, Lecture Notes in Computer Science* **8160** (2013), 145–163.
[19] H. Afrabandpey, M. Ghaffari, A. Mirzaei and M. Safayani, A novel bat algorithm based on chaos for optimization tasks, *Iranian Conference on Intelligent Systems (ICIS)* (2014), 1–6.
[20] Z. Zhou, H. Duan, P. Li and B. Di, Chaotic differential evolution approach for 3D trajectory planning of unmanned aerial vehicle, *2013 10th IEEE International Conference on Control and Automation (ICCA)*, Hangzhou, China, (Jun 12–14 2013), 368–372.
[21] M. Shirani, G. Härkegård and N. Morinb, Fatigue life prediction of components made of spheroidal graphite cast iron, *Procedia Engineering* **2**(1) (2010), 1125–1130.
[22] A.N. Celik, A statistical analysis of wind power density based on the weibull and rayleigh models at the southern region of turkey, *Renewable Energy* **29**(4) (Apr 2004), 593–604.
[23] M.A.R. de Pascoa, E.M.M. Ortega and G.M. Cordeiro, The kumaraswamy generalized gamma distribution with application in survival analysis, *Statistical Methodology* **8** (2011), 411–433.
[24] K.L. Roscoe and F. Diermanse, Effect of surge uncertainty on probabilistically computed dune erosion, *Coastal Engineering* **58** (2011), 1023–1033.
[25] A. Pillepich, C. Porciani and O. Hahn, Halo mass function and scale-dependent bias from N-body simulations with non-taussian initial conditions, *Oxford Journals of Science and Mathematics (MNRAS)* **402**(1), 191–206.
[26] E.H. Mamdani and S. Assilian, An experiment in linguistic synthesis with a fuzzy logic controller, *International Journal of Man-Machine Studies* **7** (1975), 1–13.
[27] J.H. Holland, Adaptation in natural and artificial systems: An introductory analysis with applications to biology, *Control and Artificial Intelligence*, MIT Press, USA, (1992).
[28] T. Sottinen and C.A. Tudor, On the equivalence of multiparameter Gaussian processes, *Journal of Theoretical Probability* **19**(2) (2006), 461–485.
[29] J.F. Corney and P.D. Drummond, Gaussian quantum monte carlo methods for fermions and bosons, *Physical Review Letters* **93**(26) (2004), 260401.
[30] V. Heinz and D. Knorr, High pressure inactivation kinetics of bacillus subtilis cell by a three-state model considering distributed resistance mechanisms, *Food Biotechnology* **10** (1996), 149–161.
[31] N.C. Sagias and G.K. Karagiannidis, Gaussian class multivariate weibull distributions: Theory and Applications in Fading Channels, *IEEE Transactions on Information Theory* **5**(10) (2005), 3608–3619.
[32] D.M. Deaves and I.G. Lines, On the fitting of low mean wind speed data to the Weibull distribution, *Journal of Wind Engineering and Industrial Aerodynamics* **66**(3) (Mar 1997), 169–178.
[33] G.J. Husak, J. Michaelsen and C. Funk, Use of the gamma distribution to represent monthly rainfall in Africa for drought monitoring applications, *International Journal of Climatology* **27**(7) (15 Jun 2007), 935–944,
[34] E. Furman, On a multivariate gamma distribution, *Statistics and Probability Letters* **78**(15) (2008), 2353–2360.
[35] S. Yue, A bivariate gamma distribution for use in multivariate flood frequency analysis, *Hydrological Processes* **15**(6) (30 Apr 2001), 1033–1045.
[36] G.W. Flake, The computational beauty of nature: Computer explorations of fractals, chaos, complex systems, and adaptation, MIT Press, Cambridge, Massachusetts (1998), 469–482.
[37] E. Zitzler and L. Thiele, Multiobjective optimization using evolutionary algorithms – A comparative case study, in: *Conference on Parallel Problem Solving from Nature (PPSN V)* (1998), 292–301.
[38] N. Beume, B. Naujoks and M. Emmerich, SMS-EMOA: Multiobjective selection based on dominated hypervolume, *European Journal of Operational Research* **181**(3) (2007), 1653–1669.
[39] S.K. Pradyumn, On the normal boundary intersection method for generation of efficient front, in: *ICCS 2007, Part I*, Y. Shi et al., eds, (LNCS 4487), Springer-Verlag Berlin Heidelberg, (2007), 310–317.
[40] I. Elamvazuthi, T. Ganesan and P. Vasant, A comparative study of HNN and Hybrid HNN-PSO techniques in the optimization of distributed generation (DG) power systems, *International Conference on Advanced Computer Science and Information System (ICACSIS)* (2011), 195–200.
[41] P. Vasant, I. Elamvazuthi, T. Ganesan and J.F. Webb, Iterative fuzzy optimization approach for crude oil refinery industry, *Scientific Annals of Computer Science* **8**(2) (2010), 261–280.

AUTHOR COPY

View publication stats